Application of Fail-Safe Structural Design to Piping System

Hidetoshi IBE, Tetsundo NAKATOGAWA
Mitsubishi Atomic Power Industry, Tokyo, Japan
Toshiaki HISADA, Hirohisa NOGUCHI, Osamu MURAYAMA
University of Tokyo, Tokyo, Japan
Armen Der KIUREGHIAN
University of California, Berkeley, CA USA

1.INTRODUCTION

The safety of a nuclear power plant is a most critical matter for the public. Therefore, safety devices, such as safety relief valves or rupture discs, are sometimes installed in pipelines to make sure of preventing excessive pressure. Using a similar philosophy, if a plant's structural members are designed with sufficient margin under the specified seismic design conditions, there exists a degree of uncertainty about the magnitude of the seismic loads and the strength of the members and hence we feel some difficulty in assessing the safety margin exactly. In response to this situation, we have introduced the fail-safe concept illustrated in table-1. In this concept, if the structure should fail, its overall safety will be maintained because the failure is limited to an unimportant portion of the structure. This concept makes better use of yielding or even breakage of structural members and will imply an overall improvement in the reliability and the cost of the structure.

Recognition and control of the failure mode are very important when we apply the fail-safe design concept to a structure. As a first attempt to apply this concept, we have discribed its application to the design of seismic supports for piping systems. We performed a sensitivity analysis on a typical piping system using a time history of seismic acceleration, and a dynamic non-linear FEM [1] was used for the sensitivity analysis.

From these results, we showed how to find out which parameter should be adjusted for controlling the failure mode from the sensitivity analysis process and studied how to recognize the failure mode.

2 CASE STUDY

2.1 OBJECT

A typical residual heat removal system of a PWR nuclear power plant was chosen as the model piping system. The synthetic time history seismic wave and the corresponding floor response spectra are shown in fig-1. The piping system model is shown in fig-2, and the seismic wave is applied in the x-axis direction.

The reliability of the structure depends largely on the arrangement and the characteristics of the support structures. In this case, we considered only the yielding of the support structures as the failure mode of the piping system.

2.2 DERIVATION OF FORMULAS TO EVALUATE SESITIVITIES

The sensitivities of the parameters such as yield loads can be obtained by the following formulas.

The equilibrium equation for the dynamic problem is given by

$$M\ddot{U}_i + Q_i = \sum_{l=1}^{i} F_l \tag{1}$$

where Fi is each load step, and Ui and Qi are accelerations and internal forces after the ith load step respectively. The internal force Qi may be described as follows by the tangential damping and stiffness matrices.

$$Q_i = \sum_{l=1}^{i} \left(\int_{\dot{U}_{l-1}}^{\dot{U}_l} C \, d\dot{U} + \int_{U_{l-1}}^{U_l} K \, dU \right) \tag{2}$$

Let the system parameter bj have variation dbj(= αb_j, $|\alpha| << 1$), and the corresponding mass matrix be M ,and the corresponding tangential stiffness be K , the equilibrium equation is then given as follows instead of Eq(1).

$$M_\alpha (\ddot{U}_i + \Delta \ddot{U}_i) + Q_{\alpha i} = \sum_{l=1}^{i} F_{\alpha l} \tag{3}$$

where $\Delta\ddot{U}_i$ is the total variation of the acceleration due to the perturbation of the system which is denoted by the subscript. Based on Eq(2), the perturbed internal force vector Q is given by

$$Q_{\alpha i} = \sum_{l=1}^{i-1} \left(\int_{\dot{U}_{l-1}+\Delta\dot{U}_{l-1}}^{\dot{U}_l+\Delta\dot{U}_l} C_\alpha \, d\dot{U} + \int_{U_{l-1}+\Delta U_{l-1}}^{U_l+\Delta U_l} K_\alpha \, dU \right) + \int_{\dot{U}_{i-1}+\Delta\dot{U}_{i-1}}^{\dot{U}_i} C_\alpha \, d\dot{U} + \int_{U_{i-1}+\Delta U_{i-1}}^{U_i} K_\alpha \, dU + \int_{\dot{U}_i}^{\dot{U}_i+\Delta\dot{U}_i} C_\alpha \, d\dot{U} + \int_{U_i}^{U_i+\Delta U_i} K_\alpha \, dU \tag{4}$$

The following equations for the first order variations are derived.

$$M \, \delta\ddot{U}_i + C \, \delta\dot{U}_i + K \, \delta U_i = - \delta R_i \tag{5}$$

$$\delta R_i \approx \sum_{l=1}^{i-1} \left(\int_{\dot{U}_{l-1}+\delta\dot{U}_{l-1}}^{\dot{U}_l+\delta\dot{U}_l} C_\alpha \, d\dot{U} + \int_{U_{l-1}+\delta U_{l-1}}^{U_l+\delta U_l} K_\alpha \, dU \right) + \int_{\dot{U}_{i-1}+\delta\dot{U}_{i-1}}^{\dot{U}_i} C_\alpha \, d\dot{U} + \int_{U_{i-1}+\delta U_{i-1}}^{U_i} K_\alpha \, dU - \sum_{l=1}^{i} F_{\alpha l} + M_\alpha \ddot{U}_i \tag{6}$$

As for the implicit time integration scheme, the Newmark-β method given in Eqs.(7) and (8) will be used.

$$\dot{U}_i^{(k)} = \dot{U}_{i-1} + \frac{1}{2} (\ddot{U}_{i-1} + \ddot{U}_i^{(k)}) \Delta t \tag{7}$$

$$U_i^{(k)} = U_{i-1} + \dot{U}_{i-1} \, \Delta t + \left[\left(\frac{1}{2} - \beta\right) \ddot{U}_{i-1} + \beta \ddot{U}_i^{(k)} \right] \Delta t^2 \tag{8}$$

It is noted that Δt represents the time step of integration. The components with superscript (k) are renewed in the Newton-Raphson iteration. The first order variational representation of Eqs.(7) and (8) due to the system perturbation are given as follows.

$$\delta \dot{U}_i = \delta \dot{U}_{i-1} + \frac{1}{2} (\delta \ddot{U}_{i-1} + \delta \ddot{U}_i) \Delta t \quad (9)$$

$$\delta U_i = \delta U_{i-1} + \delta \dot{U}_{i-1} \Delta t + \{ (\frac{1}{2} - \beta) \delta \ddot{U}_{i-1} + \beta \delta \ddot{U}_i \} \Delta t^2 \quad (10)$$

Substituting Eqs.(9) and (10) into Eq.(5), we have the following equation to solve for the variation of the acceleration.

$$(M + \frac{\Delta t}{2} C + \beta \Delta t^2 K) \delta \ddot{U}_i = - \delta R_i - C (\delta \dot{U}_{i-1} + \frac{1}{2} \Delta t \, \delta \ddot{U}_{i-1}) - K \{ \delta U_{i-1} + \delta \dot{U}_{i-1} \Delta t + (\frac{1}{2} - \beta) \Delta t^2 \delta \ddot{U}_{i-1} \} \quad (11)$$

As the effective stiffness matrix $(M + \frac{\Delta t}{2} C + \beta \Delta t^2 K) \equiv K^*$ in the above is the same as that of the original system, the variation $\delta \ddot{U}_i$ is easily obtained after the completion of the Newton Raphson iteration for the original system. Then $\delta \dot{U}_i$ and δU_i are simply calculated by Eqs.(9) and (10).

We can get the approximate sensitivities $\partial U_i / \partial b_j$ by dividing δU_i by δb_j.

In this case study, we neglected damping (C) and modelled the piping system with the elbow element model proposed by BATHE [3], and we have performed a sensitivity analysis. By using the elbow model, we can consider changes of stiffness due to internal pressure and the ovalization ,and also the effect of the flanges. For this case study, the number of integration points totalled 27400 for the piping system illustrated in fig-2.

2.3 SENSITIVITY ANALYSIS RESULTS

From the results of a time history analysis of the piping system, relatively high stresses emerged at the points W1 to W6 in fig-2 and the largest peak stress appeared at W3. We calculated the sensitivities of each corresponding stress (S) relative to the yield load (Fy) for every support (P1 to P10) when we performed the sensitivity analysis based on the dynamic non-linear FEM described in 2.2. For this sensitivity analysis, the characteristics of the support structures used are shown in fig-3.

The sensitivity analysis results are shown in fig-4 to fig-7. The vertical axis and the horizontal axis represent the $Fy \times \partial S / \partial Fy$ and the time respectively. The sensitivities for P1,P4,P5,P6 and P10 don't appear in these figures because P1,P4 and P10 remained in the elastic state and the sensitivities of W1, W2, W3, and W4 for P5 and P6 were very small and negligible.

In fig-4, the sensitivities of P2,P3 and P8 were large as we expected, but it should be noted that that of P7 is also not negligible small. Sensitivity of P7 is shown most notably in fig-5 and fig-6. Hence we think we can control the stresses of W2 and W3 by adjusting the yield load of the support P7. The sensitivity of many supports' yield loads on W4 stress is shown in fig-7. In this case, the stress of W4 can be apparently reduced by increasing the yield loads of supports P3 and P8 with negative sensitivities. The stresses of W4 can also be reduced by decreasing the yield load of P7.

In fig-4 to fig-7, the sensitivity of the stresses of W1 and W4 to the support P7 is significant when compared with the other supports that are closer to W1 and W4. As a result, we considered that the yield load of P7 influenced the overall piping system.

From these observation, we can recognize that we can control the failure mode of the piping system by changing the yield loads of the support structures. Also we concluded we could adjust structural the members to achieve a favorable failure mode for the fail-safe design of a system. From a designer's standpoint, what is important is the sensitivities of the reliability with respect to the design valuables. These can be obtained eventually from the reliability analysis like the following way.

2.4 RELIABILITY INDEX COMPUTATION

According to the fail-safe design concept illustrated in table-1, we indicate that the most likely failure will not occure at the critical part of a subject system that will affect the system's safety.

For example, if the yielding of W1,W2 or W3, which are located in the main pipe of this piping system, affects the system's overall safety, we need to evaluate the reliability index based on Eq.(12) for the more important part of the system and confirm that it is larger than another reliability index based on Eq.(13) for the less important part which will not affect the overall safety. Using these equations, which are called the limit state functions, we can get the reliability indices by the FORM using the CARLEL computer code[2] and their sensitivities to the design valuables.

$$P=P\,[G1<0 \cup G2<0 \cup G3<0] \qquad (12)$$

$$P=P\,[G4<0 \cup G5<0 \cup G6<0] \qquad (13)$$

where Gi=Sy-MAX[Si]
Sy=yield stress of the piping material
Si=maximum stress at Wi

If we can adjust yield loads of the support structures by watching the reliability indices, we can achieve fail-safe structural design for pipings.

3.PROSPECTS

In conclusion, we have demonstrated a fail-safe design procedure which shows how to know which parameter should be adjusted for controlling the failure mode by using the sensitivity analysis and how to recognize a failure mode by the reliability index. A part of the results of the piping study will be reported at the SMiRT 11 conference.

In this paper, we demonstrated the fail-safe design of piping support structures, but we will be able to realize the fail-safe design of the whole piping system in the same manner when we can estimate the elasto-plastic characteristic of piping material, and obtain reliability indices for pipe break conditions.

Also we believe the concept of the fail-safe design will be useful not only for a reasonable design, but also for a quality assurance, because the cause of the failure is often related to the quality of a system.

4.REFERENCES

[1] Hisada, T., Noguchi, H., Murayama,O. & Der Kiureghian,A.1990"Reliability Analysis of Elasto-Plastic Dynamic Problem"

[2] Liu, P-L, Hong-Zong Liu, Der Kiureghian, A., 1989 "Calrel User Manual" UCB/SEMM-89/18

[3] Bathe, K.J., Almeida, C.A.1980 "A Simple and Effective Pipe Elbow Element -Linear Analysis"

Table-1 Fail-safe design

	CONVENTIONAL DESIGN	FAIL-SAFE DESIGN
①DESIGN LOAD	DETERMINISTIC VALUE	PROBABILISTIC (OR REALISTIC) VALUE
②FAILURE MODE CONSIDERED	BASED ON ENGINEERING DECISION	BASED ON SENSITIVITY ANALYSIS USING NON-LINEAR FEM
③ANALYSIS METHOD	LINEAR (IN GENERAL)	NON-LINEAR
④CRITERIA	ALLOWABLE STRESS/STRAIN	RELIABILITY INDEX β or FAILURE PROBABILITY
⑤GOAL	SAFE STRUCTURE	FAIL-SAFE STRUCTURE
⑥MERIT	ENSURE SAFETY AT DESIGN CONDITION	ENSURE SAFETY AT DESIGN AND ULTIMATE SEVERE CONDITIONS CONSIDERING COST-BENEFIT

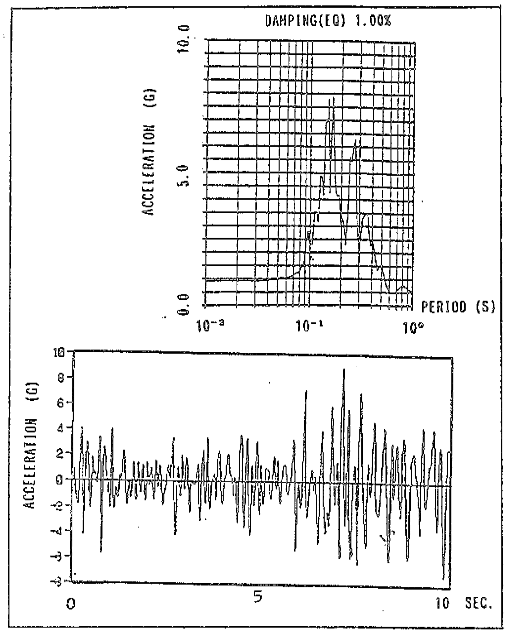

Figure-1 Assumed earthquake for case study

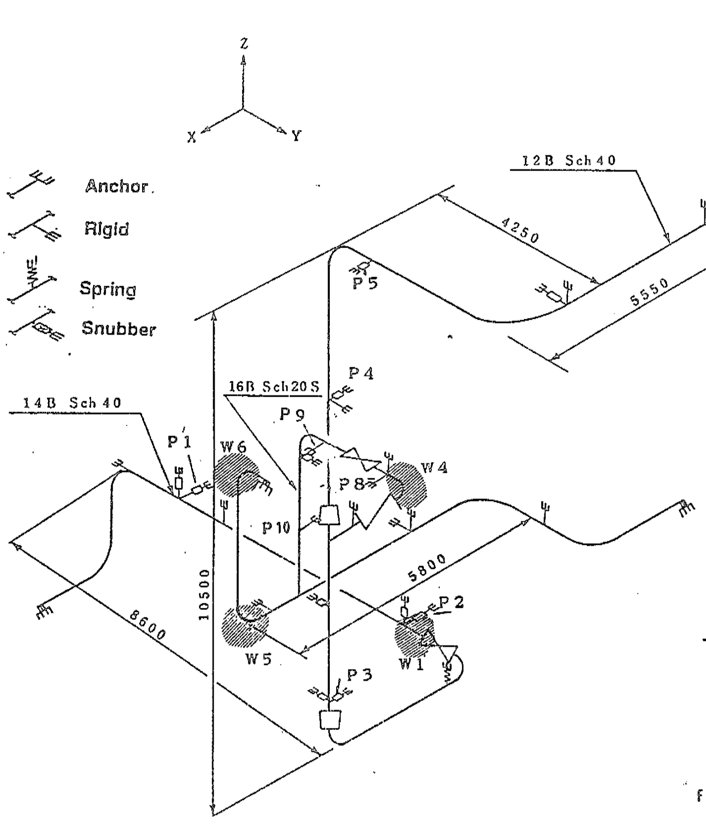
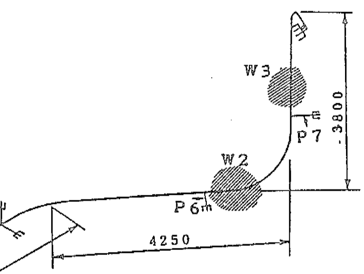

Figure-2 Sample case of piping systems

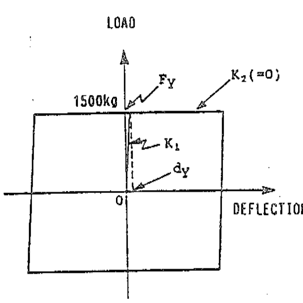

Figure-3 Assumed characteristic of support structures (P1 ~P10)

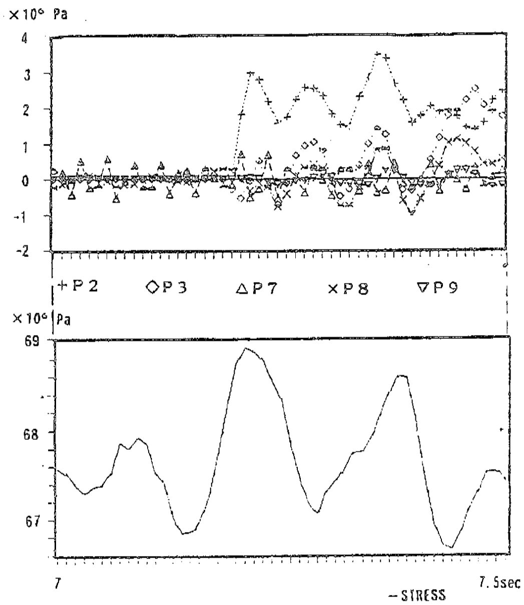

Figure-4 Sensitivity of stress at W1

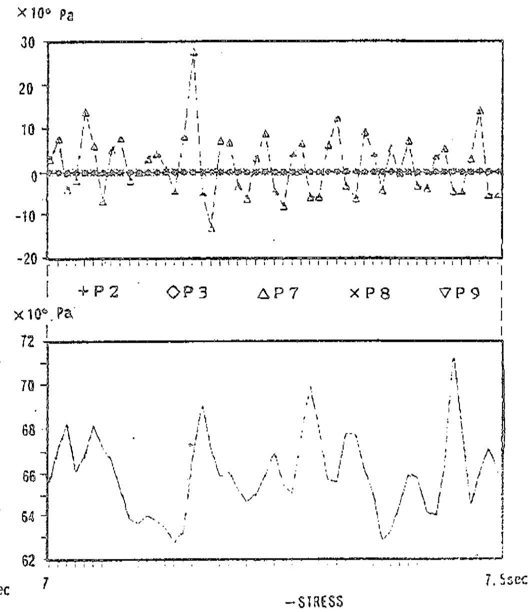

Figure-5 Sensitivity of stress at W2

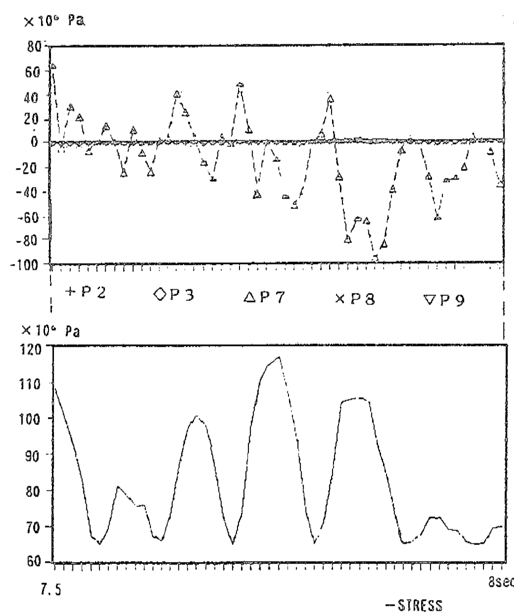

Figure-6 Sensitivity of stress at W3

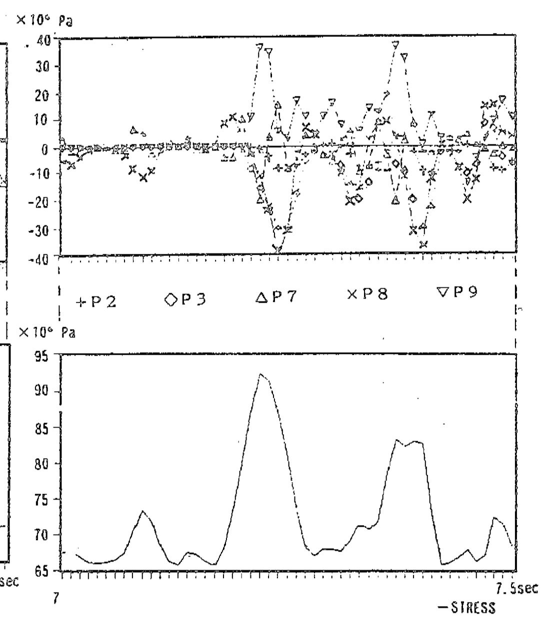

Figure-7 Sensitivity of stress at W4